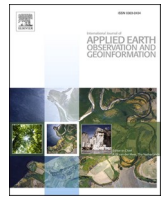


Contents lists available at ScienceDirect

International Journal of Applied Earth Observations and Geoinformation

journal homepage: www.elsevier.com/locate/jag



Seeing through the clouds – Mapping desert fog oasis ecosystems using 20 years of MODIS imagery over Peru and Chile

Justin Moat^{a,*}, Alfonso Orellana-Garcia^{b,c}, Carolina Tovar^a, Mónica Arakaki^b, César Arana^b, Asunción Cano^b, Luis Faundez^d, Martin Gardner^{e,i,j}, Paulina Hechenleitner^{a,c,e,i,j}, Josefina Hepp^{f,j}, Gwilym Lewis^a, José-Manuel Mamani^g, María Miyasiro^h, Oliver Q. Whaley^{a,c,e,i}

^a Royal Botanic Gardens, Kew, Richmond, Surrey TW9 3AE, UK

^b Universidad Nacional Mayor de San Marcos, Museo de Historia Natural and Facultad de Ciencias Biológicas, Av. Arenales 1256, Lima 11, Peru

^c Huarango Nature, Lima, Peru

^d Biota Gestión y Consultoría Ambiental Ltda., Chile

^e Royal Botanic Garden Edinburgh, 20A Inverleith Row, Edinburgh EH3 5LR, UK

^f Centro del Desierto de Atacama, Pontificia Universidad Católica de Chile, Santiago, Chile

^g Universidad Continental, Cusco, Peru

^h Proyecto para la conservación, gestión y rehabilitación de los ecosistemas frágiles de lomas en Lima (EbA Lomas) SERNANP – PNUD, Av. Jorge Chávez 275, Miraflores, Peru

ⁱ Rainforest Concern, 66 Great Pulteney Street, Bath, BA2 4DL, UK

^j Fundación Chilco, Santiago, Chile

ARTICLE INFO

Keywords:

Atacama
Google Earth Engine
Lomas
Oasis de Niebla
Remote sensing
Tillandsia

ABSTRACT

The desert fog oasis ecosystem of Peru and Chile comprises numerous oases along 3000 km of the Pacific coastal belt, it hosts a highly endemic flora, providing vital ecosystem services and genetic resources. However, due to their marked seasonality and fog cover they are poorly mapped, greatly compromising their conservation. Here we redress this using 479 images from the MODIS (MOD13Q1 V6 product) data/algorithm for the period 2000–2020, permitting the mapping of ephemeral vegetation, herbaceous and woody fog oases vegetation. In addition, we examine the main drivers of productivity in this unique ecosystem using generalised linear models, assess human pressures, conservation efforts, and summarise present plant diversity knowledge.

The resultant map (<https://gistin.users.earthengine.app/view/fog oasis>) extends existing mapped areas by more than four-fold to over 17,000 km², revealing extensive little-known vegetation habitats with few or no collection records. *Tillandsia* ('air plants') fog oases were mapped manually due to poor spectral discrimination and were found to cover an area of approximately 1,900 km² the majority of which is in Peru (96%). Fog oasis productivity is significantly related to aridity and distance to the coast, as well as elevation and slope angle. Most fog oases peak in productivity during August–September, although productivity is highly variable between August and December with different oases reacting to inter-annual and annual climate fluxes.

Only 4% of fog oases are protected, most are threatened by mining, urban development, air pollution and off-road 4 × 4 driving. Urgent action is needed to protect these areas, which we estimate support around 1200 ecosystem-specific flowering plant species with approximately 30% endemism in Peru and 67% in Chile. By presenting a comprehensive map and catalogue of Peruvian and Chilean fog oases, we hope to catalyse increased conservation and research towards a better understanding of these exceptional ecosystems within South America.

* Corresponding author.

E-mail addresses: J.Moat@kew.org (J. Moat), alfonso.orellana@unmsm.edu.pe (A. Orellana-Garcia), C.Tovar@kew.org (C. Tovar), marakakim@unmsm.edu.pe (M. Arakaki), caranab@unmsm.edu.pe (C. Arana), acanoe@unmsm.edu.pe (A. Cano), lfaundez@biota.cl (L. Faundez), MGardner@rbge.org.uk (M. Gardner), phechenleitner@rbge.org.uk (P. Hechenleitner), jnhepp@uc.cl (J. Hepp), G.Lewis@kew.org (G. Lewis), jmamani@continental.edu.pe (J.-M. Mamani), maria.miyasiro@gmail.com (M. Miyasiro), O.Whaley@kew.org (O.Q. Whaley).

1. Introduction

1.1. The desert fog oasis context

The arid coastal belt of Peru and Chile, which includes the Atacama and Sechura deserts, is one of the world's most ancient arid regions and is considered one of the driest (Hartley et al., 2005). The governing influence of marine currents, Andean uplift, and climatic extremes including ENSO (El Niño, Southern Oscillation), have produced a unique set of bioclimatic conditions, which have shaped the evolution, distribution, and productivity of the native vegetation. Seasonal advective and orographic fog supply the only significant annual moisture along this hyperarid belt 3000 km long (Cereceda et al., 2002). This marine generated fog sustains plant communities in the fog oases, known locally as "lomas" (Peru) or "oasis de niebla" (Chile). ENSO and episodic precipitation events see the area of vegetation productivity expand and contract. To date, comprehensive mapping of Peruvian and Chilean fog oases is lacking.

Functioning as ecological islands in the desert, fog oases in Peru and Chile vary widely with latitude, aspect, substrate, and elevation, ranging from hilltop woody plant refugia to wider expanses of vegetation and productive crusts. Three main fog oasis types can be identified: **1. Ephemeral fog oases** which support poorly recorded cryptobiotic (biological) crusts (Arana et al., 2016; Rengifo-Faiffer and Arana, 2019) and lichen meadows (Vargas Castillo et al., 2017; Whaley et al., 2019) and rapidly reproducing annual plant species which appear infrequently (flowering every 5 to 30 years or more), and are associated with unusually dense or penetrating fogs or highly sporadic rainfall events (Chávez et al., 2019). Here, typically, large numbers of long-lived seeds (such as *Nolana* spp.) can be found on, or close to, the surface. **2. *Tillandsia* fog oases** are composed of several long-lived perennial *Tillandsia* species (Hesse, 2012; Pinto et al., 2006; Rundel and Dillon, 1998), often forming phytogenic mounds and stabilised dunes (Hesse, 2014, 2012). *Tillandsia* patches occupy a marginal xerophytic, sandy dune niche, where moisture (from fog drip) is insufficient to cause decay of anchoring leaves and root-like structures. **3. Herbaceous and woody fog oases** are the most humid and botanically rich, composed of woody perennial shrubs (such as *Atriplex*, *Lycium*, *Frankenia*, *Ephedra*, *Proustia*, *Euphorbia*), with interspersed geophytes and annuals which produce leaves and flowers only when enough fog is available to penetrate the soil surface. These fog oases often include rock refugia rich in endemic species, including lichens, mosses and even desert ferns (Faúndez, 2018; Whaley et al., 2019). These wettest fog oases can support small trees and columnar or barrel cacti (especially from the genera *Eulychnia*, *Trichocereus*, *Copiapoa*, *Eriosyce*). Herbaceous and woody fog oases are known to be predominantly verdant during the austral winter (June to August) but perennial elements are evident throughout the year (Faúndez, 2018; Rundel et al., 1991).

1.2. The human fog oasis context

Ancient human coastal settlement from c. 10,000 BP (Beresford-Jones et al., 2015) have developed around fog oases drawing on their cultural and physical resources. Fog oases house important crop wild relatives, including those of potato, tomato, pumpkin, and papaya, as well as useful medicinal, fuel and dye plant species (Beresford-Jones et al., 2015; Dillon et al., 2011), whilst providing wildlife corridors for endangered animal species such as guanacos, desert fox, condors and pampas cat.

The importance of fog oases is being increasingly recognised; for example, in Lima, Peru, five areas have been protected as UNESCO World Heritage Sites. Nevertheless, the majority of fog oasis vegetation remains poorly known, poorly protected, and highly threatened by overgrazing, urban development (Trinidad et al., 2012), pollution (Sträter et al., 2010), 4 × 4 off-roading (Schulz et al., 2012), mining, and climate change (Schulz et al., 2012).

The research foci and information needed to protect and understand fog oases is greatly hampered by the lack of accurate maps. Here we begin to redress this need.

1.3. Delimiting the fog oases

Extensive systematic ground surveys of Peruvian fog oases were conducted by Ramón Ferreyra between the 1940's and 1990's, and in Chile, by Johnston in the 1920's, Dillon and Rundel in the 1990's and Muñoz-Schick et al., Pinto and Luebert in the 2000's. More extensive surveys have been conducted since the 1990's and, since 2015, complemented with remote sensing and Unmanned Aerial Vehicles (UAV). Notwithstanding this, fog oases remain one of the most difficult ecosystems to map and delimit. The first challenge is that fog obscures the vegetation during its growing season. Secondly, many fog oases may be verdant only for short periods each year, and the ephemeral area may only flush into full leaf once a decade or greater. Thus, mapping fog oases using optical satellites (e.g., Landsat and Sentinel) with infrequent repeat periods, short view periods and incomplete archives can be problematic. Nevertheless, Landsat (Muenschow et al., 2013b, 2013a; Paredes, 2011) Sentinel (Pauca-Tanco et al., 2020), Spot, RapidEye (Ministerio Ministerio del Ambiente, 2019) and Worldview (Beresford-Jones et al., 2015; Wolf et al., 2016) have successfully used the Normalised Difference Vegetation Index (NDVI) to differentiate the verdant fog oases. However, this has been limited to a few well-studied fog oases, when the right conditions occur (e.g., limited fog or cloud cover and vegetation in flush), and only offers a snapshot in time for relatively small areas. Thirdly, although the perennial *Tillandsia* fog oases are less obscured by fog, light diffraction and reflection from the unique trichomes covering *Tillandsia* leaves create a silver-grey appearance that hampers differentiation from the background desert (Hesse, 2012; Wolf et al., 2016). To date, only a few detailed regions of *Tillandsia* fog oases have been mapped using visual inspection (Hesse, 2012; Pinto et al., 2006) and high-resolution imagery or UAV imagery combined with pattern recognition (Wolf et al., 2016).

Due to these difficulties, the extensive mapping of fog oases has required the visual interpretation of either aerial photography (Pinto et al., 2006), or satellite imagery and Google Earth (Ministerio del Ambiente, 2019). This visual snapshot approach is prone to misinterpretation of geological and edaphic features, crucially with much of the ephemeral and physically obscured fog oases excluded, leaving them unrecognised and unprotected.

To successfully map all fog oases, and capture imagery during fog or cloud-free windows, satellite systems with long archives and very high repeat periods are required. Both the Global Inventory Modelling and Mapping Studies (GIMMS) and Moderate Resolution Imaging Spectroradiometer (MODIS) offer precisely these functions. GIMMS NDVI has been used successfully to capture the 'flowering desert' of Atacama (Chávez et al., 2019). However, due to low resolution ($\sim 85 \text{ km}^2$ area), low sensitivity and lack of recent imagery (mission ended in 2013), it is ineffective in distinguishing fog oases from other nearby vegetation types or sparse vegetation. This is the case for many of the Peruvian fog oases, which are often close to urban areas, irrigated agriculture, or riverine vegetation. MODIS, the successor to GIMMS, provides an opportunity to map fog oases in more detail over the past 20 years because of its repeat periods of 1–2 days, and red and Near Infra-Red (NIR) band at 250 m resolution (Didan et al., 2015).

For the first time, here we: 1) delimit, classify and estimate the extent of all ephemeral, woody and herbaceous fog oases in Pacific coastal South America by using the 20 year archive MODIS imagery, and extend existing research to quantify *Tillandsia* fog oases; 2) examine the ecological parameters and drivers that underlie this unique ecosystem; 3) assess the level of human pressure and the protection needed to ensure the survival of fog oases, whilst summarising the current level of ecological knowledge.

2. Material and methods

2.1. Study area

Our study area covers the Pacific coastal desert region of Peru and Chile, from 5.8° S to 28.5° S, approximately 3000 km in length and incorporating all previous fog oasis mapping and botanical studies (Fig. 1). We restrict our analysis to the area within 50 km of the western seaboard of South America, and within an altitudinal range of 25 to 1800 m asl, to capture the full range of fog oases. The lower elevation boundary of 25 m was set to remove areas of marine macroalgae. Previously, the upper boundaries of fog oases have been suggested to be approximately 1000 m (Dillon et al., 2011; Rundel et al., 1991) or 1200 m (Pinto, 2005; Schulz et al., 2012; Whaley et al., 2019), corresponding with elevational and meteorological parameters of fog formation and interception with the land.

The northern limit includes Península de Illescas (Cerro Las Cuevas, south of the city of Piura, Peru) which represents the final transition of coastal fog vegetation as it blends into equatorial dry forest scrub (Fig. 1). The southern limit is Rio Huasco and includes the coastal section of Llanos de Challe National Park, which represents the transition from fog oasis to sclerophyllous vegetation (Fig. 1). These northern and southern-most ecological transitions were classified as “Transitional fog oases”, which were treated separately and not included in the full analysis.

2.2. Datasets

2.2.1. Satellite data

We used the MOD13Q1 V6 product which gives a vegetation index value at 250 m pixel resolution every 16 days (Didan et al., 2015), and chose NDVI for our analysis due to its sensitivity in arid environments. The MODIS MOD13Q1 V6 NDVI algorithm uses the best available pixel from all time periods over 16 days, and uses an atmospherically corrected bi-directional surface reflectance masking water, clouds, dense aerosols, and cloud shadow (Didan et al., 2015). This largely eliminates issues with cloud and fog cover, which is seasonally ubiquitous in this region of coastal South America. In total we used 479 images from 18th February 2000 until 7th December 2020.

2.2.2. Botanical Inventory

We collated and georeferenced botanical data from all floristic site-specific publications for each fog oasis, 71 sites in Peru and 18 in Chile (Fig. 1), derived from 82 publications. These included peer-review journals, new species descriptions, dissertations, online databases, checklists, and herbarium specimen labels. With the aim of quantifying the plant diversity of fog oases alone, we filtered out species not associated with fog oasis ecosystems, such as riparian and dry forest species, that had been included in multiple habitat checklists. We also filtered out taxa only identified to genus level, as well as introduced and cultivated species, leaving native fog oasis habitat species only.

2.2.3. Additional data

Several sources of additional data were used to either help with fog oases delimitation, as control or to analyse the resultant maps. These data are summarised in suppl. Table S1.

All datasets were resampled in R (R Core Team, 2016) to the same extent and resolution (250 m) as the resultant MODIS imagery (see suppl. material S1 for code and data).

2.3. Analysis

2.3.1. Mapping of fog oases

We used Google Earth Engine (GEE) (Gorelick et al., 2017) to process the MOD13Q1 V6 imagery (Didan et al., 2015) to identify verdant fog oases. We used two NDVI values to delimit fog oases categories: > 0.15

for herbaceous and woody fog oases (hereafter core verdant fog oases), which after testing showed good differentiation (compared to the National Map of Ecosystems of Peru (Ministerio del Ambiente, 2019), fieldwork and authors expert knowledge of specific localities), with very little noise, matching the same threshold suggested by Chávez et al. (2019). Additionally, we used a lower threshold of 0.1 up to 0.15 to define the sparse and ephemeral vegetation. For each 16-day period the images were processed to give two binary images; each of these 16-day images (479 in all) were then summed to give the number of 16-day periods (since February 2000) where the vegetation was above the 0.1 or 0.15 NDVI threshold. These two final images were classified by the average percentage cover period during which the vegetation was verdant (over the last 20 years), giving us 6 verdant fog oasis classes (Table 1).

In addition to verdant fog oases, our remote sensing analysis identified cultivated areas, riverine vegetation (usually irrigated), and xerophytic habitat on lower slopes of the western Andes. We tested several methods to automatically discard these areas, but none proved accurate enough and were too problematic for later analysis (e.g., removing some altitudes would cause systematic error in further analyses). Therefore, we visually examined all these areas masking non-fog oases areas from the analysis (see suppl. material S1 for code and data).

Tillandsia fog oases remain elusive to the more traditional remote sensing techniques. Therefore, to assess their approximate extent we identified regional occurrences from existing literature (Hesse, 2012; Oka and Ogawa, 1984; Pauca-Tanco et al., 2020; Pinto, 2005; Pinto et al., 2006; Whaley et al., 2019; Douglas, 2017) and hand-digitised formations based on their distinctive ripple and cluster patterns (Hesse, 2012; Wolf et al., 2016) using Google Earth imagery. Additionally, sites were identified and verified using georeferenced herbarium specimens and observations of oasis-forming *Tillandsia* species (*T. geissei*, *T. landbeckii*, *T. latifolia*, *T. marconae*, *T. tragophoba*, and *T. purpurea*). Digitised polygons and the more detailed mapping for the Ica region (Hesse, 2012) were simplified and smoothed to the same scale as ephemeral and core verdant fog oasis areas to account for the greater ambiguity and lower density of some *Tillandsia* fog oases.

2.3.2. Comparison to existing surveys

Previous mapping of fog oases has been highly problematic and, as a result, only well-known fog oases are mapped in the National Map of Ecosystems of Peru (Ministerio del Ambiente, 2019). This, combined with the accumulative methods (twenty years of data) of our analysis, the ephemeral nature of the vegetation and high fog and cloud cover, made more traditional accuracy assessment (i.e., presence and absence at a point in time) impractical. Our resultant maps and results have been extensively verified by the authors by: (1) using author's expert knowledge and data from previous fieldwork (from the 1990's onwards) to verify particularly fog oases in central and southern Peru and northern Chile and (2) using Google Earth imagery. Additionally, to give an indication of congruence, we calculated the overlap between our map and lomas identified in the National Map of Ecosystems of Peru.

2.3.3. Environmental drivers of fog oases

To test the significance of the environmental variables, as drivers of verdant fog oases, (using the number of 16-day periods where NDVI was above 0.15 as a response variable), we randomly sampled 30,000 points across all mapped verdant fog oases. Due to the lack of quantified measurements of fog moisture intercepted by plants across the landscape, we used aridity index, annual temperature, latitude, distance from the coastline, aspect, elevation, and slope (radians) as explanatory variables (suppl. table S1). Most of the variables had a normal distribution curve except for aridity. As elevation and temperature are highly correlated, we selected elevation as the key determinant of fog oases, as it was of higher accuracy than temperature datasets. Likewise, precipitation was excluded in the analysis as datasets are poor for this hyperarid region. Because the response variable has positive integer values, we

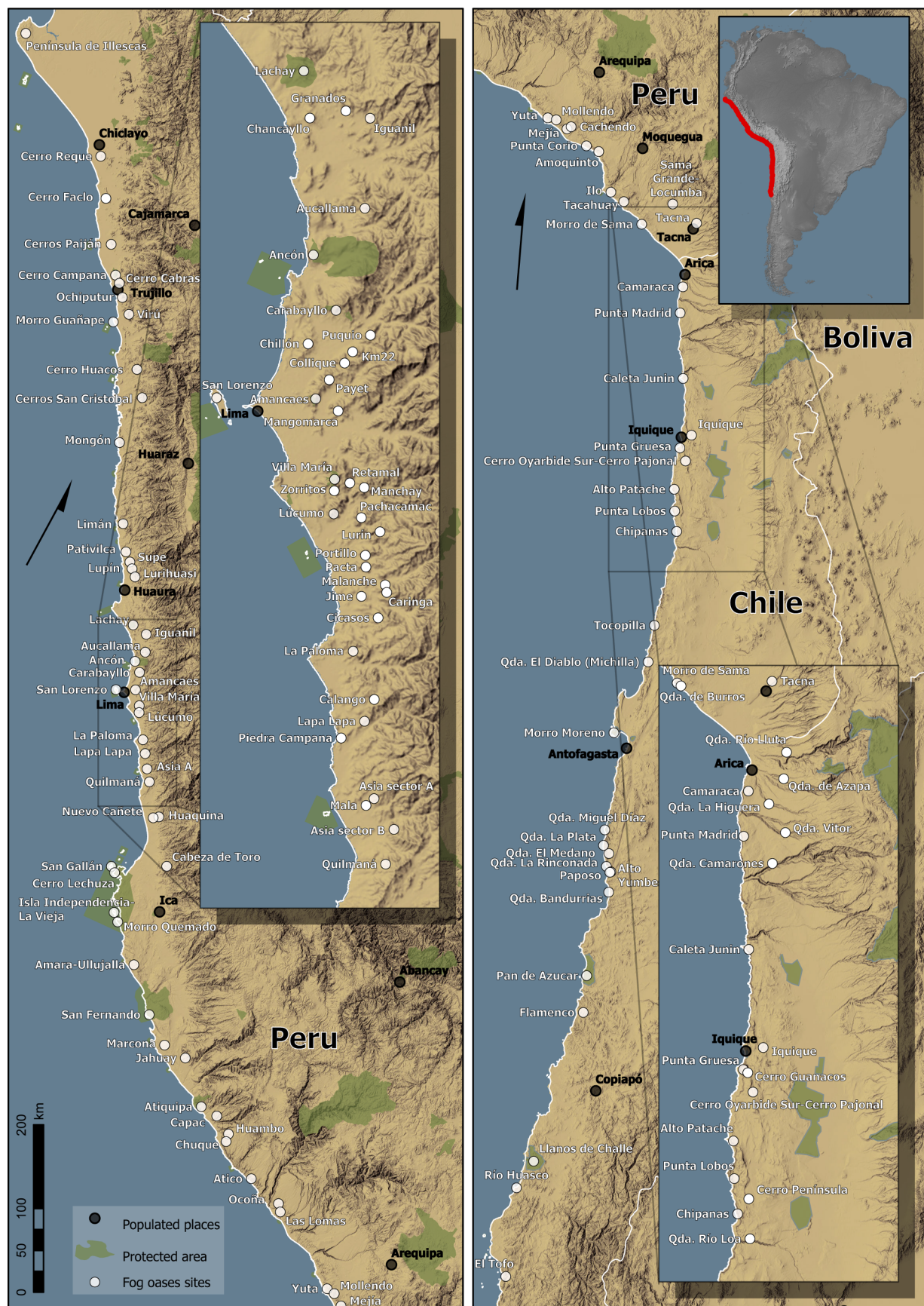


Fig. 1. Map of fog oasis sites (botanical collection sites) and protected areas of Peru and Chile. See <https://gistin.users.earthengine.app/view/fog oasis> for interactive and detailed maps.

Table 1

Verdant Fog oases classification (ephemeral vs herbaceous and woody fog oases) based on NDVI value and verdant period.

Class	Percentage period verdant over the last 20 years (yearly mean period in brackets)	NDVI value	Fog oasis categories and nomenclature used within this paper
1	< 2% (<1 week)	> 0.1 & < 0.15	Ephemeral fog oases
2	2–4% (1–2 weeks)	> 0.15	
3	4–8% (2–4 weeks)	> 0.15	
4	8–25% (1–3 months)	> 0.15	Core verdant fog oases (i.e., herbaceous, and woody fog oases)
5	25–50% (3–6 months)	> 0.15	
6	> 50% (>6 months)	> 0.15	Verdant oases

chose a generalised linear model with a negative binomial distribution. Assumptions of normality and homogeneity of variance were met (see [suppl. material S2](#) for details). We used the R package MASS (Modern Applied Statistics with S) and the function `glm.nb` ([Venables and Ripley, 2003](#)) ([suppl. material S1](#) for code).

2.3.4. Characterisation of verdant fog oases

We grouped each patch of fog oasis based on its relative isolation. Larger patches (approximately 50 km in length - in some cases larger) were further split using suitable geographic features (i.e., quebradas (ravines or gorges)) or when recognised as a botanical hotspot delimited in the literature. This was performed in ArcGIS Pro 2.7 using the fog oases map exported from GEE. This gave us 60 tangible units (regions) for the summary analysis and visualisation. We obtained the summary statistics of fog oasis extent, aridity index, elevation, distance from coast, and slope ([suppl. Figure S1](#)) for each of the 60 regions using the R raster package ([Hijmans, 2020](#)) and the zonal function. Data was either exported for cartographic visualisation in ArcGIS Pro 2.7 or analysed in R ([R Core Team, 2016](#)) using boxplots for all the continuous datasets, and bar charts for the categorical data utilising `ggplot` ([Wickham, 2016](#)).

Additionally, seasonality (duration of season and peak month), isolation, human pressure, protection and approximate number of plant species were also summarised per region. Seasonality was reviewed by collating mean monthly NDVI values for each region's core verdant fog oasis corresponding pixels in GEE. Isolation was estimated by measuring the distance to the nearest neighbour verdant core, directly to the North and South, or North West and South East (depending on the coastline orientation), allowing us to derive the isolation distance and the direction to the closest area. We excluded fog oases with core areas below 2 km² from this analysis. Human pressure was assessed by extracting the values from the global human footprint (HFP) map ([Venter et al., 2016](#)) within a 10 km buffer around the fog oases (all classes) within a region, to gather data from the surrounding environs. The 10 km buffer represents an easily accessible area (i.e., 2 h walking or a short drive). Percentages of protected fog oases were analysed using national maps (Peru: [SERNANP, 2019](#); Chile: [UNEP-WCMC, 2020](#)). Finally, we collated all the botanical data into these 60 geographic units.

2.3.5. Presentation and mapping of results

We have assigned a name and unique number (1 to 60), running north to south, for the identified fog oasis regions, with numbers placed in square brackets after the locality name. We use this in all results, the discussion, and figures (i.e., San Fernando [28]).

Most fog oases are in fact complexes, often with several names for distinct hills and topographical units within them. Many are in Spanish and others have ancient pre-Columbian origins. A comprehensive list of fog oasis sites, referred to in the botanical literature and on herbarium labels, are collated along with protected areas in [Fig. 1](#) (see [suppl. material S1](#)). We include additional local names derived from fieldwork, online maps and [GeoNames \(2020\)](#).

As many fog oases are too small to discern on the printed page map (given the 3,000 km total extent), we present the results as larger polygons, extracted from a 50 km coastline strip buffer - these are not used for the analysis, just for visualisation.

For wider application and use, we provide our results and maps as a Google Earth Engine app (see <https://gstin.users.earthengine.app/view/fog oasis>), where the reader can zoom into details and interact with the data.

For cartographic presentation, we used South American Equidistance Conic map projection, but rotated it by –28 for single maps and –31 and –10° for double maps to give an optimum print orientation. Colours and palettes were largely based from the recommendations of [Harrower and Brewer, 2003](#) and map production using ArcGIS Pro 2.7.

3. Results

3.1. Mapping fog oases

We identified 17,093 km² of verdant fog oases, of which, 8,678 km² are core verdant fog oases, while 8,414 km² are ephemeral fog oases ([Table 2](#)). We also identified 6,575 km² of transitional verdant fog oases. Peru has the largest area of core verdant fog oases at 80% of the total (6,964 km²) and Chile has 20% (1,714 km²) ([Figs. 2, 3, Table 2](#) and [suppl. Figure S1](#)). Of these core fog oasis areas, there are over 900 discrete patches, ranging from a few hectares (our smallest mapping unit being 0.0625 km²) to the very large contiguous fog oases of: Paposo norte to Quebrada Cascabeles - Cifuncho [52–54] in Chile which is over 610 km², and Complejo Quilmaná [22] in Peru which is over 420 km². The arid divide ([Rundel et al., 1997](#)) is evident between Peru and Chile as a climatic disjunction between Morro de Sama [41] and Complejo Arica [42], and continues to Antofagasta (Morro Moreno y Chimba [50]), with only small fog oasis patches persisting over a distance of >600 km ([Fig. 2](#)). There are, however, important *Tillandsia* fog oases in these regions.

In total we have identified an area of approximately 1,900 km² of *Tillandsia* fog oases, of this the majority (96%) occurs in Peru ([Table 2](#)). Extensive areas of *Tillandsia* oasis are highlighted in the Ica region [27–29] and Tacna [41], areas of 642 km² and 306 km² respectively ([Figs. 2 and 3](#) and [suppl. Figure S1](#)).

3.2. Comparison of our fog oases map to existing maps

To assess the quality of our analysis, we overlaid previously identified and mapped verdant fog oases (or *lomas*) from the National Map of Ecosystems of Peru ([Ministerio del Ambiente, 2019](#)), this identifies 3,060 km² of *lomas* fog oases. This is a significant contrast to our verdant fog oases total of 12,052 km² for Peru. Of the 3,060 km² previously mapped, 94% coincides with our results. Visual inspection of the areas of discrepancy showed that the majority were due to the cartographic scales of the ecosystem maps (1:2.2 million) with simplified polygons compared to the resolution of MODIS.

3.3. Environmental drivers of fog oases

The GLM results ([suppl. material S2](#)) show positive significant relationships between the number of 16-day periods where NDVI is above 0.15, elevation, aridity (note higher aridity index equates to less aridity), latitude (note higher values represent the northern areas) and slope (all

Table 2

Summary of the areas of fog oases in Peru and Chile (km^2). See Fig. 3 for summary by region. Period lengths (in brackets) are the mean time over the last 20 years.

	Class	Peru		Chile		Fog oases total	
		Fog Oases	Transitional Fog Oases	Fog Oases	Transitional Fog Oases	Fog Oasis	Transitional Fog Oases
	Ephemeral < 2% (<1 week)	5,088	61	3,327	2,371	8,414	2,432
Core	2 - 4% (1 - 2 weeks)	1,096	145	447	1,017	1,543	1,162
	4 - 8% (2 - 4 weeks)	1,135	251	479	1,321	1,613	1,572
	8 - 25% (1 - 3 months)	1,744	232	466	975	2,210	1,207
	25 - 50% (3 - 6 months)	1,357	38	174	135	1,531	173
	> 50% (> 6 months)	1,631	12	148	17	1,780	30
	Verdant Core	6,964	677	1,714	3,466	8,678	4,144
	Verdant (all)	12,052	738	5,041	5,837	17,093	6,575
	Tillandsia	1,836		71		1,907	

with P values of $< 2e-16$). Significantly, negative relationships are observed for distance to coast. Aspect also shows a significant positive relationship, but its influence is lower than for the other variables.

3.4. Fog oases characterisation

In the following section we report on the verdant fog oases only (not the transitional fog oases). Results are summarised in Fig. 3 and suppl. material Figure S2. The transitional fog oases results are represented in these figures for consistency, context, and comparison. Due to the greater ambiguity of the *Tillandsia* fog oases we only report on the area protected.

3.4.1. Climate and geographic characterisation

Nearly all fog oases exist in the hyperarid zone (Fig. 3), with the mean aridity often well below the < 0.05 hyperarid threshold (Midleton and Thomas, 1997). Lomas de Lachay [16] is an exception to this, with a mean index of 0.0672 (less arid). Most fog oases occur at a mean elevation of 500 m, but some significant areas can reach greater elevations (e.g., Sama Grande y Locumba [40] at a mean height of 824 m, and Arequipa [31] at mean elevation of 735 m, but reaching a maximum of 1800 m).

The distance from fog oases to the coastline (Fig. 3) is predominantly driven by the topography of Andean uplift, which in turn determines the distance from marine currents and the width of the coastal plain. Most Chilean fog oases [41–58] are coastal, whereas Peruvian fog oases range from close to the coast to several kilometres inland. There are notable exceptions to this: Complejo Cerro Reque [2], Cerros de Santa [8], Cerros Nepeña (norte) [10], Complejo El Carmen, Chincha [24], Jahuay (Acari) [30], Sama Grande y Locumba [40] with mean distances from the coast of 22, 25, 26, 26, 25 and 41 km, respectively.

Slope inclination of the fog oases is dominated (72%) by moderate to strong slopes ($5^\circ - 16.5^\circ$). Gentle slopes ($> 5^\circ$) occur in 12% of the fog oases and generally represent stabilised sand dunes (e.g., Lomas de Marcona [29]) or the highly ephemeral fog oases. A remaining 17% of fog oases are in the very strong ($> 16.5^\circ$) slope inclination category, representing the steep, coastal fog oases of Chile [42–44, 47–49, 51, 52] and two coastal areas in Peru [9, 32]. As would be expected, in most cases the mean aspect of fog oases, is predominantly seaward, towards the south westerly prevailing wind (Fig. 3) which drives fog formation (the marine inversion layer). A few exceptions to this occur as exceedingly small patches of vegetation determined by topographic features which produce fog eddies, or where “fingers” of fog penetrate inland along ravines.

3.4.2. Seasonality and isolation

Most fog oases (65%) have a peak productivity in August (38%) and September (26%) but, overall, productivity varies greatly between August and December. There are many notable exceptions (Fig. 3), with the northernmost fog oases [1–4] peaking in early austral autumn (March) (noting this ecological transition area also corresponds with unreliable seasonal precipitation). Lomas San Fernando [28] and Jahuay [30] have mean productivity peaks in the austral summer (December to February).

The isolation results reveal three major, somewhat contiguous, fog oasis zones - with only small distances between them (< 10 km). The first, 480 km long, runs from Casma through Lima to Sunampe [14–23] just north of Paracas in Peru. The second, 520 km long, in southern Peru, begins at Arequipa [31] and continues to the Peru-Chile border [41]. The third, in Chile, running from Paposo [52–58] merges into the transitional fog oases [59–60] and is 300 km in length. Also highlighted are the highly isolated fog oases in Ica [27, 28], Peru and Alto Patache [46] and Antofagasta [50], Chile.

3.4.3. Human pressure and protection

The HFP analysis indicates that fog oases within Peru have the highest anthropogenic pressures; the HFP is at its most extreme around Lima [17–20] and the northern cities of Chiclayo, Trujillo, and Chimbote [2, 3, 5], with a HFP index of up to 33.5 (50 is the global maximum). Conversely, the low population density in northern Chile is reflected in the low human footprint values, with only some higher values around Iquique [45] and Antofagasta [50].

Significantly, only 4% of the core verdant fog oases (Peru 3.3%, Chile 7.1%) are within a classified protected area (Figs. 1 and 3).

3.4.4. Botanical surveys and checklists

Our collection and literature review revealed over 1722 plant taxa associated with fog oases in Peru and Chile. Approximately 19% were identified only to genus level, and several undescribed species and infraspecific taxa are suspected.

After discounting these unidentified taxa, introduced, cultivated and non-fog oases plants, we estimate approximately 1200 native flowering plants are specifically and evolutionarily associated with fog oases. Of these, approximately 675 species occur in Peru, and 630 in Chile, with around 105 species occurring in both countries. Plant endemism levels are about 30% in Peru and 67% in Chile, with an overall endemism level for fog oases at around 52%. Approximately 81 non-flowering plants are recorded, but we suggest that lichens and mosses, especially, are vastly under collected.

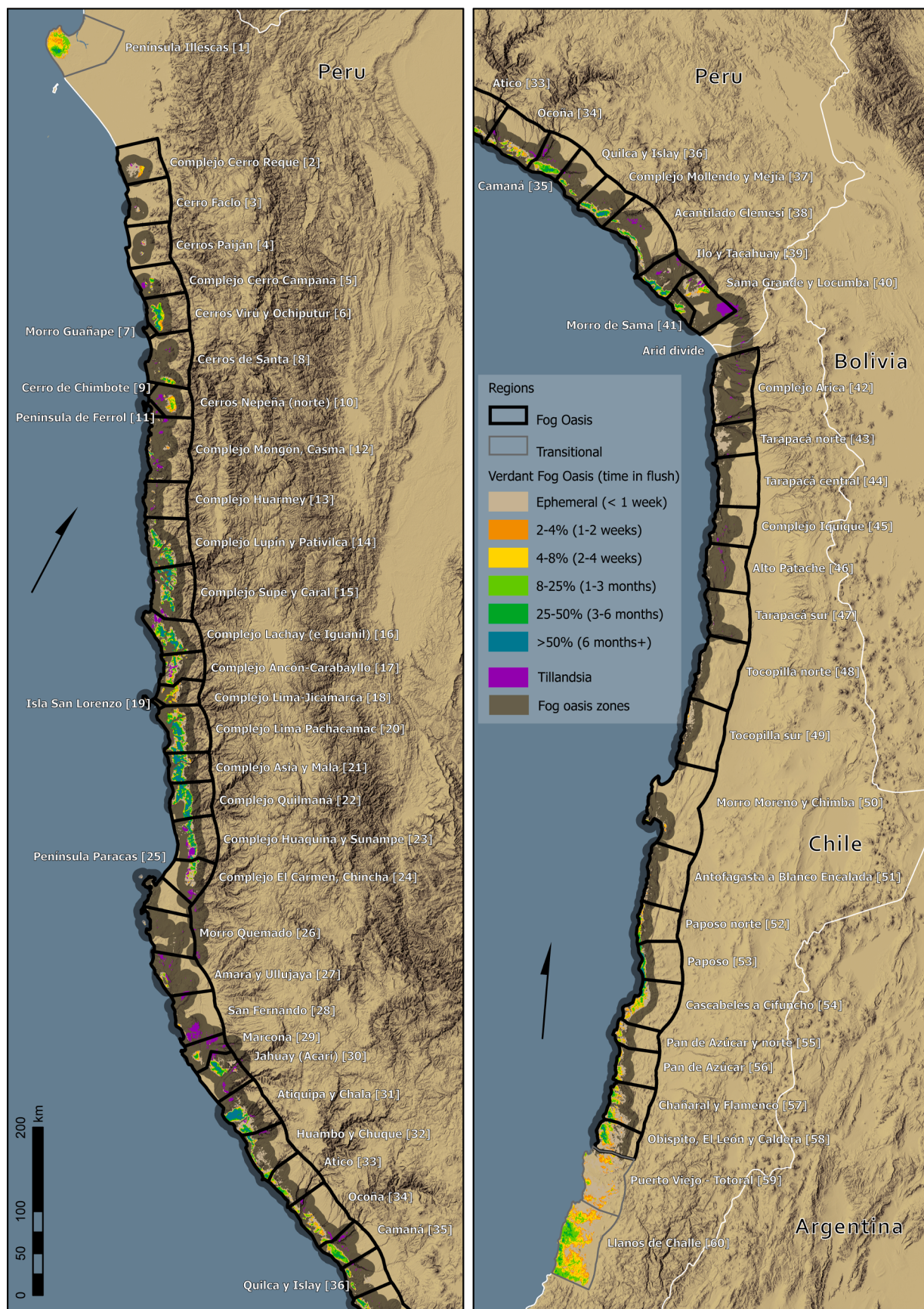
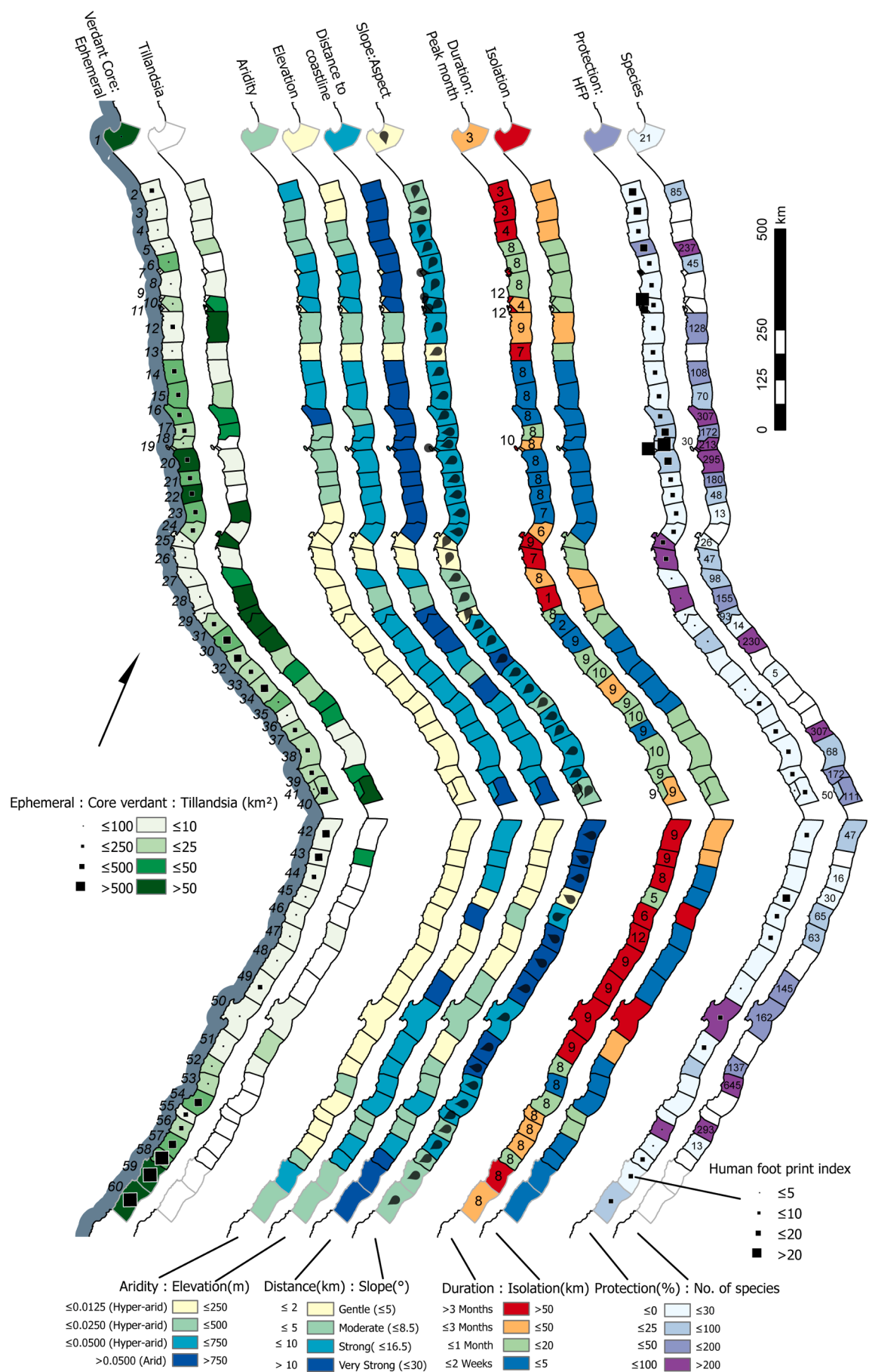


Fig. 2. Map of the verdant and *Tillandsia* fog oases of Peru and Chile, names are given as unique region identifiers, 1 to 60. A 10 km shade zone has been applied to the fog oases to highlight smaller areas beyond print resolution. Transitional areas are not highlighted. See <https://gistin.users.earthengine.app/view/fog oasis> for higher resolution and interactive mapped data. N.B. maps rotated -31° and -10° from north.



(caption on next page)

Fig. 3. Summary Infographic of fog oases characteristics. Left to right: **Extent (shades of green)**, area of core verdant oasis (km^2), area of ephemeral verdant oasis (square symbol size indicates proportion), area of *Tillandsia* fog oasis (km^2). **Characteristics (shades of blue)**: aridity index, elevation (m), distance from coastline (km), slope angle (degrees), slope direction (arrows show direction). Analysis (red to blue): duration of season ($\text{NDVI} > 0.15$), peak month (as number), isolation (km). **Impacts and knowledge (shades of purple to blue-grey)**: protection (% of protected area), human footprint (global scale of 0–50) and approximate number of plant species recorded. N.B. maps rotated -28° from north. (For interpretation of the references to colour in this figure legend, the reader is referred to the web version of this article.)

We collated the approximate number of species recorded in each fog oasis (including those non-ecosystem specific), in the 60 major regions, highlighting significant gaps in collecting (Fig. 3). The fog oases hotspot in Chile with the standout highest number of plants is Paposo [53] (632 spp. total with 460 native and 280 endemics) followed by Pan de Azucar [56] (293 spp.). In Peru, the highest number of plant species is found in Lomas de Lachay [16] (261 spp.), followed by Cerro Campana [5] (236 spp.). The centre of fog oasis diversity south of Lima, is Lomas de Atiquipa [31] (230 spp.). There are an additional seven fog oases with over 150 species each and a further 15 fog oases with over 100 species.

We found around 95 introduced species recorded in fog oases, including several aggressive invasives such as *Tamarix* sp. and *Tribulus terrestris*. Peru has approximately 71 introduced species and Chile 76, of which 20 species occur in both countries. Notably, fog oases in Peru had at least 21 cultivated species whilst none were recorded for Chile.

4. Discussion

4.1. Verdant fog oases

The 20-year archive of MODIS data, consolidated into 16-day summaries, has allowed us to see through gaps between clouds and fog, which is extremely difficult with higher resolution orbiting satellites with low repeat periods (16 and 12 days), and a single time of day capture (e.g., Landsat or Sentinel). Whilst it is difficult to assess the complete accuracy, we achieved 94% agreement with existing fog oasis maps of ecosystems of Peru and extended the previously known mapped areas more than four-fold. Without the application of satellite analysis during a two decade period (herein), Dillon (1997) estimated that Peru's lomas vegetation covers an area of less than $2,000 \text{ km}^2$, whilst Rundel et al. (1997), suggested an area of no greater than $4,000 \text{ km}^2$ for Peru and Chile combined. Our results show that this figure is closer to $12,000 \text{ km}^2$ for Peru, and over $17,000 \text{ km}^2$ for Chile and Peru combined (Table 2). Therefore within both Peru and Chile, the full extent of fog oases is revealed to be much greater than previously thought, with an additional $6,575 \text{ km}^2$ of mixed habitat transitional fog oases also identified. It should be noted that within our study we are measuring the total extent over a 20-year period (i.e., accumulative), which will therefore capture a much higher vegetation extent compared to data for any one year or event. This data has allowed us to demonstrate three major zones (connected regions) of verdant fog oasis (individual areas with $< 10 \text{ km}$ separation). Moreover, there are many isolated fog oases separated by distances as large as 150 km .

4.2. *Tillandsia* fog oases

The remote sensing of *Tillandsia* fog oases with traditional spectral methods is difficult, due to low spectral discrimination of *Tillandsia* from the background landscape (Hesse, 2012). Whilst a NDVI response was detected from *Tillandsia* areas occasionally, it is likely, as our ground surveys revealed, that at most of these areas a small number of annual herbaceous species are reacting to sporadic increases in moisture within the *Tillandsia* vegetation. Our simple visual mapping using Google Earth, with ground-truthing where possible, has identified approximately $1,900 \text{ km}^2$ of *Tillandsia* fog oases along the Pacific coast. Whilst this gives an indication of the overall extent, we advise some caution, given the difficulties in delimitation over huge areas and the challenge (as outlined above) of distinguishing *Tillandsia* fog oases from surrounding

geomorphology. Also, to a lesser extent, ground-truthing has revealed that some areas of *Tillandsia* fog oases are no longer alive but are formations of dead plants preserved by the hyperaridity (Hesse, 2012; Pinto, 2005).

Our method, and those suggested by Hesse (2012), are based on diagnostic *Tillandsia* growth pattern formations in the landscape. Wolf et al. (2016) extended this through use of high resolution imagery (UAV's and Worldview-2) with pattern analysis, demonstrating that *Tillandsia* vegetation can be successfully delimited, albeit at small scale. With the increasing availability of high-resolution imagery and use of UAVs (Baena et al., 2018), we hope this will stimulate further research into this extensive, yet poorly known ecosystem.

4.3. Characteristics and drivers of the verdant fog oases

Our extensive analysis of the temporal magnitude of fog oasis vegetation has allowed us to investigate the characteristics of the verdant fog oasis. Our results show that fog oases generally occur between elevations of $50\text{--}1000 \text{ m asl}$ (mean 500 m) on the hills and slopes facing the prevailing wind (usually South to South Westerly) and the Pacific Ocean, developing on moderate to strong slopes (5° to 16.5°) and within reach of the coast (mean distance 9.5 km). Our driver analysis corroborates these observations and shows that the more persistent and verdant fog oases occur optimally: at higher elevation (with lower temperatures), with lower aridity (higher aridity index, but still within hyperarid), on steeper slopes, and generally located towards the more northern latitudes and closer to the coastline. Slope aspect does show a significant relationship with NDVI, but not as strong as the other variables assessed; this may be driven by the scale of our analysis (reported aspect is greatly influenced by pixel scale, especially in rough terrain, (Mukherjee et al., 2013)), but also by the topographically determined wind flow at ground level. The local terrain, and vegetation at structural fine scale, will greatly influence the wind direction and moisture loading. The dominant wind direction is altered by the topography, which is analogous to river flow with turbulence; wind funnels and eddies through the terrain produce significant microclimatic changes and alters habitat niche patterns.

The fog oases peak productivity is identified as tracking the foggiest months with the austral winter (June, July and August) (Rundel et al., 1991). During the 20-year period we used, we found that in the majority of fog oases (65%), peak productivity occurs slightly later in August and September, which agrees with Pinto et al. (2005). However, we also found atypical seasonality patterns for certain fog oases. For example, two of the Ica lomas, San Fernando [28] and Jahuay [30] (Fig. 4a) are unusual in having their peak productivity in January and February, respectively, whilst the northernmost fog oases [2–4] have vegetation peaks in March (coinciding with seasonal showers). These seasonally atypical fog oases are usually located where localised sea currents have an influence over the dominant Humboldt current and produce complex unpredictable counter-currents (Chaigneau et al., 2013). In addition, many fog oases have non-typical years of peak productivity outside their usual season (Ferreyyra, 1993); these are represented as outliers in the yearly NDVI boxplots (examples in Fig. 4).

We have outlined the environmental characteristics of “typical” fog oases, but there are many exceptions and outliers. This is accentuated by fluxes in seasonality patterns within fog oases, which are much more complex than previously thought. Further research and monitoring are needed to gain a better understanding of the interactions of terrain,

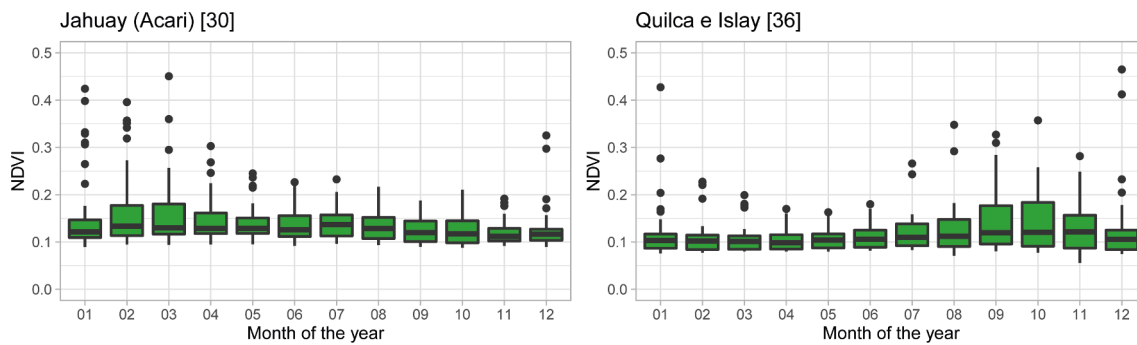


Fig. 4. a) Boxplots of monthly NDVI values for an atypical fog oasis Jahuay (Acari) [30] and b) a more typical fog oasis Quilca e Islay [36], showing many outlying months (dots beyond the whiskers) with strong vegetation vigour outside the typical fog oasis months (August and September).

wind, ocean currents and ocean temperatures in fog formation, and its interception with the vegetation and landscape. ENSO events produce large rainfall occurrences on the Peruvian coast and in northern Chile, increasing in extent and productivity (Ferreira, 1993; Tovar et al., 2018). A recent study showed that Villa María, in Metropolitan Lima [20], usually 22 km² of vegetation, increased to over 40 km² during the extreme El Niño event of 1997–98 (Miyasiro and Ortiz, 2016).

4.4. Human pressures and protection

Fog oases are perhaps the most climate-responsive ecosystem on earth and are significantly altered by past human interaction (Beresford-Jones et al., 2015). They appear to be in rapid decline due to human induced climate change, as witnessed by a drier period in Chile's hyperarid coastal zone (Schulz et al., 2012). Today there are numerous and increasing pressures on fog oases; about 58% of the population of Peru live in the coastal zones near fog oases (lomas). The human footprint analysis shows the highest anthropogenic pressures are around major cities, typically in northern Peru and the capital Lima. These fog oases bordering urban areas are already reduced to higher mean elevations than is typical, and, as historical plant collection records demonstrate, previously extended much further towards the coast. The fog oases of Villa María in metropolitan Lima lost 26.3% (585 ha) between 1986 and 2014 due to urban expansion, and a further 3% (76 ha) was lost to mining (Miyasiro and Ortiz, 2016).

Besides urban expansion and mining, other activities also threaten fog oases. For example, off-roading is extremely damaging in these fragile desert environments, destroying habitats, as well as opening permanent roads, destroying biocrusts and leaving detritus and permanent scars in the landscape. The Ministerio del Medio Ambiente (MMA, 2018) also cites several severe threats to fog oases in Chile including: the presence of invasive alien species (donkeys, goats, and invasive plants) and the extraction of plants for human use.

Presently, only 4% of fog oases (4% verdant and 3.7% *Tillandsia*) is under any type of formal protection. This compares unfavourably with the 13.3% and 37.6% total protected terrestrial area for Peru and Chile, respectively (UNEP-WCMC, 2020). In addition, protected fog oasis areas are often designated to preserve marine environments or archaeological sites, and do not consider the vegetation and its ephemeral biodiversity. Nevertheless, outside formal protected areas, several local regional communities have made efforts to protect their adjacent fog oases, as in the case of San Juan de Aucallama [17], Asia [21] and Atiquipa [31] where a community administration of conservation, research and ecotourism has been established. Likewise, in metropolitan Lima, volunteers and neighbouring residents have organised themselves to promote conservation through ecotourism, such as the emblematic case of Lomas de Lúcumo [20].

4.5. Botanical surveys and biodiversity

Peruvian and Chilean fog oases habitats support at least 1200 flowering plant species specific to them (674 in Peru and 630 in Chile); of these we estimate the average level of plant endemism at 52% (30% Peru and 67% Chile). Our analysis of Chilean endemics found at least 359 species (85%) exclusively endemic to fog oases. This extraordinary endemism of plants is compelling evidence for the ancient evolution of fog oases, under climatic island-like isolation; an attribute which is particularly evident in Chile with over 420 fog oasis endemic plant species. Of huge concern, is that over a quarter of these unique endemic species (28% Chile (Faúndez, 2018) and 28% in the Ica region (Whaley et al., 2019) appear threatened with extinction. Many species have yet to be catalogued or assessed with respect to their conservation status, and we would expect the percentage of species threatened with extinction to be much higher. In addition, several new angiosperm species are described from Peru and Chile each year from fog oases, and the total number of angiosperms can be expected to increase significantly.

Given the widespread occurrence and under-collection of lichens and mosses, liverworts, and hornworts, total species numbers of these under collected groups are likely to be significantly higher.

The number of introduced species, including invasives, is symptomatic of the long-term use of fog oases for livestock, providing valuable seasonal forage. Many fog oases are devoid of protection from grazing cows and goats, and as such, are already highly degraded. The abandoned cultivation terraces (e.g., Lomas de Atiquipa [31]) reveal that fog oases have supported agriculture since pre-Columbian times; and fog oasis checklists are indicative of this, including over 20 cultivated species in Peru, whilst being notably absent in Chile where fog oases are more isolated and disconnected from the Andean escarpments.

5. Conclusions

We have been very successful with our objectives to delimit the fog oases, mapping both the verdant (herbaceous and woody vegetation 8,700 km²) and the ephemeral (8,400 km²), and *Tillandsia* fog oasis (1,900 km²). We have examined the drivers, assessed the risks and protection, and summarised the current level of ecological knowledge.

The fog oases of Peru and Chile are seasonal, ecologically isolated ecosystems, they are often thought of as relatively simple fog delineated environments, dominated by the Humboldt current and successive El Niño and La Niña events. But, as we have shown, there are few “typical” fog oases, many are isolated and extraordinarily complex, influenced by multiple factors of terrain, climate, and marine temperature fluctuation. Fog oases have provided many ecosystem services since humans arrived on the Pacific coast of South America over 10,000 years ago, and today under the threats of climate change, food poverty and water shortage, fog oases will play an increasingly vital role. Additionally, because they are highly sensitive to small fluctuations in climatic and marine

conditions, somewhat akin to coral reefs, they provide a vital ‘early warning’ system for monitoring terrestrial response to climate change and ENSO. Although there is an increasing awareness of these ecosystems, they remain under-represented in the international literature, little monitored, and are poorly represented in the protection networks (only 4% within formal protection).

The methods we have applied to map the fog oases are conceptually simple. They have drawn on terabytes of data, whose processing and downloading would have taken, until recently, prohibitive computing power and time to process. The use of Google Earth Engine, with a few lines of code has changed this, allowing data processing in near real time. This has meant that the tweaking of thresholds and visualisation of the results were realised in seconds rather than weeks, months or even years. The 20-year archive of MODIS data is invaluable for many studies, but, as we have shown, it is particularly beneficial for areas of high fog coverage and ephemeral vegetation. Using the data from the past 20 years, we have been able to capture several major vegetation events, but there will remain some areas of ‘dormant’ fog oasis (both verdant and *Tillandsia*), which will only react to exceptional and stronger localised events with longer time intervals than the 20 years of our study. These exceptional events may be evolutionary drivers of speciation by allowing temporary ecological and genetic exchange with partial unification of some of the more isolated fog oases.

The maps we present here, increase our understanding of fog oasis vegetation, and provide the baseline spatial data needed to ensure their protection and appreciate their true landscape value. Emerging technologies have allowed us to have been extraordinarily successful in mapping the verdant fog oasis using MODIS data and GEE, increasing the area of mapped fog oases four-fold, with 94% congruence with existing maps. The increasing numbers of high to medium resolution satellites with their inclusive archives, provide much promise for the future. The combination of Landsat and the Sentinel satellites with an aggregated repeat period of 5 days, could be used to produce 15 m resolution imagery from 2015 onwards.

Fog oasis productivity is significantly related to aridity and distance to the coastline, as well as higher elevation and slope angle. We have identified 1200 flowering plant species which are typical of fog oases and of these 52% are thought to be strictly fog oasis endemics. Of the plants species within the areas that have been assessed, 28% of species are threatened with extinction. Many species have not been assessed and many more species are only now being discovered.

Whilst our mapping of herbaceous fog oases has been successful, the *Tillandsia* fog oases remain somewhat elusive for spectral remote sensing; from our simple visual mapping we estimate that this mono-dominant vegetation occurs in approximately 1,900 km². Higher resolution imagery married with pattern recognition algorithms offer next generation solutions for mapping of *Tillandsia* fog oases.

We suggest that an international effort is required to urgently monitor and protect fog oases, to protect invaluable genetic resources, coastal fisheries and ecosystems that harbour the majority of biodiversity in a vast desert biome. Future studies of the 3,000 km long highly evolved hyper-responsive fog oasis ecosystem will also help to inform and predict ENSO and climate change.

CRediT authorship contribution statement

Justin Moat: Conceptualization, Methodology, Software, Validation, Formal analysis, Investigation, Data curation, Writing – original draft, Writing - review & editing, Visualization, Project administration, Funding acquisition. **Alfonso Orellana-García:** Validation, Data curation, Writing - review & editing, Supervision. **Carolina Tovar:** Methodology, Software, Validation, Formal analysis, Writing - review & editing, Visualization. **Mónica Arakaki:** Validation, Writing - review & editing. **César Arana:** Validation, Writing - review & editing. **Asunción Cano:** Validation, Writing - review & editing. **Luis Faundez:** Validation, Writing - review & editing. **Martin Gardner:** Validation, Writing -

review & editing. **Paulina Hechenleitner:** Validation, Writing - review & editing. **Josefina Hepp:** Validation, Writing - review & editing. **Gwilym Lewis:** Validation, Writing - review & editing. **José-Manuel Mamani:** Validation, Writing - review & editing. **María Miyasiro:** Data curation, Validation, Writing - review & editing. **Oliver Whaley:** Methodology, Validation, Formal analysis, Investigation, Data curation, Writing – original draft, Writing - review & editing, Project administration, Funding acquisition, Supervision.

Declaration of Competing Interest

The authors declare that they have no known competing financial interests or personal relationships that could have appeared to influence the work reported in this paper.

Acknowledgements

We are extremely grateful for the continued support from the Bentham-Moxon Trust, who funded collaborative field work in the fog oases for some of the authors. The initial investigation was supported by the UK Government’s Darwin Initiative (Project Ref. No. 15-016), and funding from Royal Botanic Gardens, Kew; J Sainsbury’s plc, and Sociedad Agrícola Samaca S.A.C. Further work is funded by the National Geographic Society (NGS-72454C-20)

This work has been gestating for many years and has only been possible through the support of many colleagues. We are grateful to Amanda Cooper, Steve Bachman, Tim Wilkinson, Bente Klitgaard and Susana Baena (all, from the Royal Botanic Gardens, Kew) for their support in the field with mapping and Red Listing of species. We thank Ian Ondo for his statistical knowledge and advice with the driver analysis, and Ralf Hesse for supplying *Tillandsia* mapping data for the Ica region. Also, to David Beresford-Jones (Archeobotanist at University of Cambridge), and Gunnar Øvstebo (Horticulturist at Royal Botanic Garden Edinburgh). To Michael Dillon (The Field Museum) for his love of fog oases and Nolana and other lomas flora we are greatly indebted.

In Perú, research and fieldwork would have been impossible without the collaboration and support of our superb project partners, especially: Asociación para la Niñez y su Ambiente-ANIA (Joaquín Leguía, Marycarmen Arteaga), Agrícola Chapi S.A. (Augusto, Ursula and Alvaro Baertl), Horizonte Corporativo (Tirco Rojas), Fundo Orgánico Huaquina-Vivero Topará (Klaus[†] and Stefan Bederski) and Samaca Orgánico (Alberto Benavides to whom deep gratitude goes for his support and love of lomas). To public and academic institutions, especially: Administración Técnica Forestal y de Fauna Silvestre (ATFFS Ica, especially to Carmen Castilla, Jhon Fernandez and Luis Mercado) of Servicio Nacional Forestal y de Fauna Silvestre (SERFOR), Servicio Nacional de Áreas Naturales Protegidas por el Estado (SERNANP; to the ANP: RNSF, RNP, RNSIIPG, RNL, ZRI, ACRSLL, ACPLA, ACPLCC.). To the Faculty of Biological Sciences and Research Institute of the San Luis Gonzaga National University (UNSLG), to the Floristics Laboratory, Botany Department of the Natural History Museum of the Universidad Nacional Mayor de San Marcos (UNMSM) and the herbarium collections at USM, MOL (Forestal and Weberbauer), HSP, HUSA, and HUT. C. Arana was partially funded by VRIP-UNMSM (Project B17100051)

We are extremely grateful to the students and professionals who have supported field collections and georeferencing of botanical data, especially: Jean Capcha, Willinton Taquiri, Iomar Santana, Christian Padilla, Emilio Mitacc, Hudson Yonjoy, Miguel Aparcana, Francisco Perales, Arlyne Ramos, Ronal Sumiano, Jesús Ormeño, Darwin Garcia, Luis Casma, Caesar Choza, Yannet Quispe, Mijahel Lara, Erick Ramírez, Josué Cárdenas, Marco Mendoza, Juan Muchaypiña, Delsy Trujillo, Daniel Montesinos, Víctor Quipuscoa, Aldo Ortega, Amalia Delgado, Norton Cuba, Roobert Jimenez, Manolo Fernandez, Ivan Reyna, Miguel Astocaza, Marco Sánchez, Fátima Cáceres[†], Miguel Hinojosa, César Cáceres Félix Quinteros, Miguel Bailetti, Emerson Ccoyllo and Jorge Chipa.

And also, huge thanks to the Área de Conservación Privada Lomas de Atiquipa directed by the Comunidad Campesina de Yauca, Jaqui y Atiquipa.

In Chile, we are grateful for the continual support of the following institutions: the National Agricultural Research Institute - INIA, especially the Seed Bank and the team led by Carolina Pañitrur (including Ana Sandoval and Sergio Ibañez); the Ministry of Environment, especially the Regional Secretariat of Antofagasta and Roberto Villablanca; the National Forestry Corporation - CONAF (in particular CONAF Atacama, Tarapacá and Antofagasta); the Atacama Desert Centre of Universidad Católica de Chile, who provided information and access to their experimental station at the Alto Patache fog oasis; and the National Research and Development Agency (ANID), for the grants and funding that have enabled this research and field visits to be carried out. A large part of the Chilean flora data set is a legacy of the 2002–2005 Darwin Initiative project (DR 11-012) collaboration between the Royal Botanic Garden Edinburgh (RBGE) and the Universidad Austral de Chile (UACH), which utilised historical herbarium collections deposited at RBGE and eventually led to the development of the Endemic plants of Chile portal. We are extremely grateful to CONAF, their staff and park rangers, for granting permission to undertake research in government protected (SNASPE) areas. We are also grateful to Juan Larraín for valuable information on the poorly known Bryophyte flora of fog oases.

Appendix A. Supplementary material

Supplementary data to this article can be found online at <https://doi.org/10.1016/j.jag.2021.102468>.

References

- Arana, C., Carlo, T.A., Salinas, L., 2016. Biological soil crust in Peru: first record and description. *Zo. Áridas* 112–116. <https://doi.org/10.21704/za.v1i61.632>.
- Baena, S., Boyd, D.S., Moat, J., 2018. UAVs in pursuit of plant conservation - Real world experiences. 47, 2–9. <https://doi.org/10.1016/j.ecoinf.2017.11.001>.
- Beresford-Jones, D., Pullen, A.G., Whaley, O.Q., Moat, J., Chauca, G., Cadwallader, L., Arce, S., Orellana, A., Alarcón, C., Gorriti, M., Maita, P.K., Sturt, F., Dupeyron, A., Huaman, O., Lane, K.J., French, C., 2015. Re-evaluating the resource potential of lomas fog oasis environments for Preceramic hunter-gatherers under past ENSO modes on the south coast of Peru. *Quat. Sci. Rev.* 129, 196–215. <https://doi.org/10.1016/j.quascirev.2015.10.025>.
- Cereceda, P., Osses, P., Larraín, H., Farías, M., Lagos, M., Pinto, R., Schemenauer, R.S., 2002. Advective, orographic and radiation fog in the Tarapacá region. *Chile. Atmos. Res.* 64 (1–4), 261–271. [https://doi.org/10.1016/S0169-8095\(02\)00097-2](https://doi.org/10.1016/S0169-8095(02)00097-2).
- Chaigneau, A., Dominguez, N., Eldin, G., Vasquez, L., Flores, R., Grados, C., Echevin, V., 2013. Near-coastal circulation in the Northern Humboldt Current System from shipboard ADCP data. *J. Geophys. Res. Ocean.* 118 (10), 5251–5266. <https://doi.org/10.1002/jgrc.20328>.
- Chávez, R.O., Moreira-Muñoz, A., Galleguillos, M., Olea, M., Aguayo, J., Latín, A., Aguilera-Betti, I., Muñoz, A.A., Manríquez, H., 2019. GIMMS NDVI time series reveal the extent, duration, and intensity of “blooming desert” events in the hyper-arid Atacama Desert, Northern Chile. *Int. J. Appl. Earth Obs. Geoinf.* 76, 193–203. <https://doi.org/10.1016/j.jag.2018.11.013>.
- Didan, K., Munoz, A.B., Solano, R., Huete, A., 2015. MODIS Vegetation Index User's Guide (Collection 6) 2015, 31.
- Dillon, M.O., 1997. *Lomas Formations - Peru*. In: *Centres of Plant Diversity. Information Press, Oxford, A Guide and Strategy for Their Conservation*. WWF, pp. 519–527.
- Dillon, M.O., Leiva-González, S., Zapata-Cruz, M., Lezama-Arceno, P., Quipuscoa-Silvestre, V., 2011. Floristic Checklist of the Peruvian Lomas Formations - Catálogo florístico de las Lomas peruanas. *Arnaldoa* 18 (1), 7–32.
- Douglas, M., 2017. Reserva Nacional Lomas de Ancon, Peru – THE NATURALIST'S TRAVEL PAGE [WWW Document]. URL <https://thetravelingnaturalist.org/ancon-reserve-peru/> (accessed 18.21).
- Faúndez, L., 2018. Biodiversidad del desierto de Atacama y estepa altiplánica. In: Figueroa, A., Rovira, J., Flores, S., Tala, C., Aviles, R., Orellana, J.L., Ferreyra, J., Diaz, P., Cohen, R. (Eds.), *Biodiversidad de Chile. Patrimonio y Desafíos*, Ministerio del Medio Ambiente (MMA), tercera edición, tomo 2. Santiago de Chile, pp. 29–40.
- Ferreyra, R., 1993. Registros de la vegetación en la costa peruana en relación con el fenómeno El Niño. *Bull. Inst. fr. études Andin.* 22, 259–266.
- GeoNames, 2020. GeoNames geographical database [WWW Document]. URL <https://www.geonames.org/> (accessed 4.30.21).
- Gorelick, N., Hancher, M., Dixon, M., Ilyushchenko, S., Thau, D., Moore, R., 2017. Google Earth Engine: Planetary-scale geospatial analysis for everyone. *Remote Sens. Environ.* 202, 18–27. <https://doi.org/10.1016/j.rse.2017.06.031>.
- Hartley, A.J., Chong, G., Houston, J., Mather, A.E., 2005. 150 million years of climatic stability: Evidence from the Atacama Desert, northern Chile. *J. Geol. Soc. London.* 162, 421–424. <https://doi.org/10.1144/0016-764904-071>.
- Hesse, R., 2012. Spatial distribution of and topographic controls on *Tillandsia* fog vegetation in coastal southern Peru: Remote sensing and modelling. *J. Arid Environ.* 78, 33–40. <https://doi.org/10.1016/j.jaridenv.2011.11.006>.
- Hesse, R., 2014. Three-dimensional vegetation structure of *Tillandsia latifolia* on a coppice dune. *J. Arid Environ.* 109, 23–30. <https://doi.org/10.1016/j.jaridenv.2014.05.001>.
- Harrower, M., Brewer, C.A., 2003. ColorBrewer.org: an online tool for selecting colour schemes for maps. *The Cartographic Journal* 40 (1), 27–37. <https://colorbrewer2.org/>.
- Hijmans, R.J., 2020. raster: Geographic Data Analysis and Modeling.
- Middleton, N.J., Thomas, D.S.G., 1997. World Atlas of Desertification. In: *Earth Surface Processes and Landforms*, , 3rd24. Arnold, London, pp. 2–7. [https://onlinelibrary.wiley.com/doi/10.1002/\(SICI\)1096-9837\(199903\)24:3%3C280:AID-ESP955%3E3.0.CO;2-7](https://onlinelibrary.wiley.com/doi/10.1002/(SICI)1096-9837(199903)24:3%3C280:AID-ESP955%3E3.0.CO;2-7).
- Miyasiro, M.G., Ortiz, M.A., 2016. Estimación mediante la teledetección de la variación de la cobertura vegetal en las lomas del distrito de Villa María del Triunfo por la expansión urbana y minera (1986–2014). Licentiate Thesis, Universidad Nacional Mayor de San Marcos, San Marcos, Peru. <https://cybertesis.unmsm.edu.pe/handle/20.500.12672/5281>.
- MMA, 2018. Aprueba Plan de Recuperación, Conservación y Gestión de la Flora Costera del Norte. Promulgación 13 de marzo de 2018. D.O. No. 42210. Ministerio del Medio Ambiente, Santiago, Chile. <https://www.bcn.cl/leychile/navegar?idNorma=1125687&idParte=0>.
- Muenchow, J., Bräuning, A., Rodríguez, E.F., von Wehrden, H., 2013a. Predictive mapping of species richness and plant species' distributions of a peruvian fog oasis along an altitudinal gradient. *Biotropica* 45 (5), 557–566. <https://doi.org/10.1111/btp.2013.45.issue-510.1111/btp.12049>.
- Muenchow, J., Bräuning, A., Rodríguez, E.F., von Wehrden, H., 2013b. Soil texture and altitude, respectively, largely determine the floristic gradient of the most diverse fog oasis in the Peruvian desert. *J. Trop. Ecol.* 29 (5), 427–438. <https://doi.org/10.1017/S0266467413000436>.
- Ministerio del Ambiente, 2019. Mapa de Ecosistemas del Perú: Memoria descriptiva [WWW Document]. URL https://cdn.www.gob.pe/uploads/document/file/309735/Memoria_descriptiva_mapa_Nacional_de_Ecosistemas.pdf & [http://geoservidor\[minam.gob.pe/wp-content/uploads/2019/01/MAPA-NACIONAL-DE-ECOSISTEMAS.zip](http://geoservidor[minam.gob.pe/wp-content/uploads/2019/01/MAPA-NACIONAL-DE-ECOSISTEMAS.zip) (accessed 4.30.21).
- Mukherjee, Samadrita, Mukherjee, Sandip, Garg, R.D., Bhardwaj, A., Raju, P.L.N., 2013. Evaluation of topographic index in relation to terrain roughness and DEM grid spacing. *J. Earth Syst. Sci.* 122, 869–886. <https://doi.org/10.1007/s12040-013-0292-0>.
- Oka, S., Ogawa, H., 1984. Distribution of Lomas vegetation and its environments along the Pacific coast of Peru. *Geogr. Reports Tokyo Metrop. Univ.* 19, 113–125.
- Paredes, R.S.M., 2011. El Niño Southern Oscillation And Its Effect On Fog Oases Along The Peruvian And Chilean Coastal Deserts. Università di Bologna.
- Pauca-Tanco, G.A., Villasante Benavides, J.F., Villegas Paredes, L., Luque Fernandez, C. R., Quispe Turpo, J.del P., 2020. Distribución y caracterización de las comunidades de *Tillandsia* (Bromeliaceae) en el sur de Perú y su relación con la altitud, pendiente y orientación. *Ecosistemas* 29. <https://doi.org/10.7818/ECOS.2035>.
- Pinto, R., 2005. *Tillandsia del norte de Chile y del extremo sur de Perú. FlorAtacama, Santiago de Chile*.
- Pinto, R., Barría, I., Marquet, P.A., 2006. Geographical distribution of *Tillandsia* lomas in the Atacama Desert, northern Chile. *J. Arid Environ.* 65 (4), 543–552. <https://doi.org/10.1016/j.jaridenv.2005.08.015>.
- R Core Team, 2016. R: A language and environment for statistical computing.
- Rengifo-Faiffer, Cristina, Arana, Cesar, 2019. Fossiliferous birds help shape the plant community of a Peruvian desert. *Journal of Arid Environments* 29–33. <https://doi.org/10.1016/j.jaridenv.2019.104011>.
- Rundel, P.W., Dillon, M.O., 1998. Ecological patterns in the Bromeliaceae of the lomas formations of Coastal Chile and Peru. *Plant Systematics and Evolution* 212 (3), 261–278. <https://doi.org/10.1007/BF01089742>.
- Rundel, P.W., Dillon, M.O., Palma, B., Mooney, H.A., Gulmon, S.L., Ehleringer, J.R., 1991. The phytogeography and ecology of the coastal Atacama and Peruvian Deserts. *Aliso* 13 (1), 1–49. <https://doi.org/10.5642/aliso10.5642/aliso.19911301.02>.
- Rundel, P.W., Villagra, P.E., Dillon, M.O., Roig-Juñent, S., Debandi, G., 1997. Arid and Semi-Arid Ecosystems. In: Veblin, T., Young, K., Orme, A. (Eds.), *The Physical Geography of South America*. Oxford University Press, Oxford, p. 1997.
- Schulz, N., Boisier, J.P., Aceituno, P., 2012. Climate change along the arid coast of northern Chile. *Int. J. Climatol.* 32 (12), 1803–1814. <https://doi.org/10.1002/joc.2395>.
- SENRANP, 2019. GEO ANP - Visor de las Áreas Naturales Protegidas [WWW Document]. accessed 4.30.21. <https://geo.sernanp.gob.pe/visorsernarp/>.
- Stráter, Ellen, Westbeld, Anna, Klemm, Otto, 2010. Pollution in coastal fog at Alto Patache, Northern Chile. *Environ. Sci. Pollut. Res.* 17 (9), 1563–1573. <https://doi.org/10.1007/s11356-010-0343-x>.
- Tovar, Carolina, Sánchez Infantas, Edgar, Teixeira Roth, Vanessa, 2018. Plant community dynamics of lomas fog oasis of Central Peru after the extreme precipitation caused by the 1997–98 El Niño event. *PLoS One* 13 (1), e0190572. <https://doi.org/10.1371/journal.pone.0190572>.
- Trinidad, H., Huamán-Melo, E., Delgado, A., Cano, A., 2012. Flora vascular de las lomas de Villa Marfa y Amancaes, Lima. Perú. *Rev. Peru. Biol.* 19, 149–158. <https://doi.org/10.15381/rpb.v19i2.834>.
- UNEP-WCMC, 2020. Protected Area Profile for Chile from the World Database of Protected Areas [WWW Document]. URL <https://www.protectedplanet.net/country/CHL> (accessed 5.1.20).

- Vargas Castillo, R., Stanton, D., Nelson, P.R., 2017. Aportes al conocimiento de la biota líquenica del oasis de neblina de Alto Patache, Desierto de Atacama. Revista de Geografía Norte Grande 68, 49–64. https://scielo.conicyt.cl/scielo.php?pid=S0718-34022017000300049&script=sci_arttext&tlang=e.
- Venables, W.N., Ripley, B.D., 2003. *Modern Applied Statistics with S*. Springer Science & Business Media, New York.
- Venter, O., Sanderson, E., Magrach, A., Allan, J., Beher, J., Jones, K., Possingham, H.P., Laurance, W.F., Wood, P., Fekete, B.M., Levy, M.A., Watson, J.E.M., 2016. Global terrestrial Human Footprint maps for 1993 and 2009. Sci. Data 3 (1). <https://doi.org/10.1038/sdata.2016.67>.
- Whaley, O.Q., Orellana-Garcia, A., Pecho-Quispe, J.O., 2019. An Annotated Checklist to Vascular Flora of the ICA Region, Peru—with notes on endemic species, habitat, climate and agrobiodiversity. Phytotaxa 389 (1), 1–125. <https://doi.org/10.11646/phytotaxa.389.110.11646/phytotaxa.389.1.1>.
- Wickham, H., 2016. *ggplot2: Elegant Graphics for Data Analysis*. Springer-Verlag, New York.
- Wolf, N., Siegmund, A., Del Río, C., Osses, P., García, J.L., 2016. Remote Sensing-Based Detection and Spatial Pattern Analysis for Geo-ecological Niche Modelling of *Tillandsia* spp. In: In the Atacama, Chile., The International Archives of the Photogrammetry, Remote Sensing and Spatial Information Sciences. Prague, Czech Republic. Prague. <https://doi.org/10.5194/isprsarchives-XLI-B2-251-2016>.